

Characterization of the Components of a Scintillation Dosimeter Prototype for Brachytherapy

N.H. Boughaba^{1, a)}, M. Martinez-Roig^{2, b)}, N. Yahlali^{2, c)}, J. Díaz^{2, d)}
and B. Bouzid^{1, e)}

¹*SNIRM Laboratory, USTHB, BP 32 El-Alia, 16111, Bab-Ezzouar, Algiers, Algeria*

²*Instituto de Física Corpuscular (IFIC), CSIC-University of Valencia, Spain*

^{a)} Corresponding author: nor-el-houdal@hotmail.fr

^{b)} Marcos.Martinez@ific.uv.es

^{c)} nadia.yahlali@uv.es

^{d)} jose.diaz@uv.es

^{e)} bbouzid@usthb.dz

Abstract. In-vivo dosimetry for brachytherapy has been investigated since decades with a number of different detectors and measurement technologies. X-ray films, semiconductor detectors, thermo-luminescent dosimeters and ionization chambers are the contemporary systems mostly used. However, ionization chambers do not allow point-like dose measurements near the tumor, semiconductor detectors are not water equivalent and are very sensitive to temperature changes, and thermo-luminescent dosimeters do not allow real-time measurements. For these reasons, during the last two decades, there has been an increased interest for scintillation dosimetry using scintillating fibers, due to their most favorable characteristics and dosimetric properties, as water equivalence, response linearity with increasing dose rates, independence from temperature and small size. In the present work, we present experimental studies of key characteristics of the components of a scintillation dosimeter: the light collection in different types of scintillating fibers and the gain as a function of temperature of a silicon photomultiplier (SiPM), for the design and construction of an in-vivo scintillation dosimeter prototype for brachytherapy.

INTRODUCTION

During high dose brachytherapy treatment, the precise measurement of the radiation delivered to solid tumors by radioactive seeds is necessary to ensure the verification and adequacy of the doses prescribed to patients, calculated by treatment planning systems (TPS) [1,2]. Currently, the use of specific in-vivo dosimeters during brachytherapy treatments is not wide spread in the clinical practice. The reason for this insufficiency is the limited availability of specific dosimetry instruments of reliable and easy use during the clinical practice. One possible solution is the plastic scintillation detectors, which have appropriate features for in-vivo brachytherapy dosimetry, as water equivalence, stability, reduced dimensions that allow point-like dose measurements and response linearity [3]. Over the last ten years, many results have been published, mainly by Beddar et al. [3-7], where scintillating fiber detectors coupled to an optical light guide were investigated and coupled to a photodetector, mainly a photodiode or a photomultiplier tube (PMT). For the development of a dosimeter for brachytherapy treatment, based on a scintillating fiber and a silicon photomultiplier (SiPM) or Multi-Pixel Photon Counter (MPPC), we present a study of key characteristics of these detector components, namely the light transmission performance of different scintillating fiber types at increasing input light intensities, and the gain stabilization procedure against variations due to temperature changes in the SiPM.

EXPERIMENTAL SETUP

Silicon Photomultiplier: Gain Study

The use of a SiPM instead of a conventional photomultiplier tube(PMT) offers many advantages for a scintillation dosimeter, such as low operating voltage ($V_{OP} < 100V$) at room temperature and with simple readout circuit, high gain (typically $\sim 10^6$) similar to PMTs, excellent spatial resolution (down to $\sim 1mm^2$), robustness and insensitivity to magnetic fields [8]. SiPM structure consists of a matrix of several hundreds to several thousands of microcells or pixels per mm^2 . Each pixel is made up of a silicon p-n junction avalanche photodiode(APD) operated in Geiger mode i.e. the SiPM is biased above the breakdown voltage V_{BD} of the junction. All pixels are connected in series with their quenching resistor R_q and in parallel to a common output where the signals are summed, as shown in Fig. 1. This sum signal gives information on the number of photoelectrons detected and the incident number of photons on the photodetector.

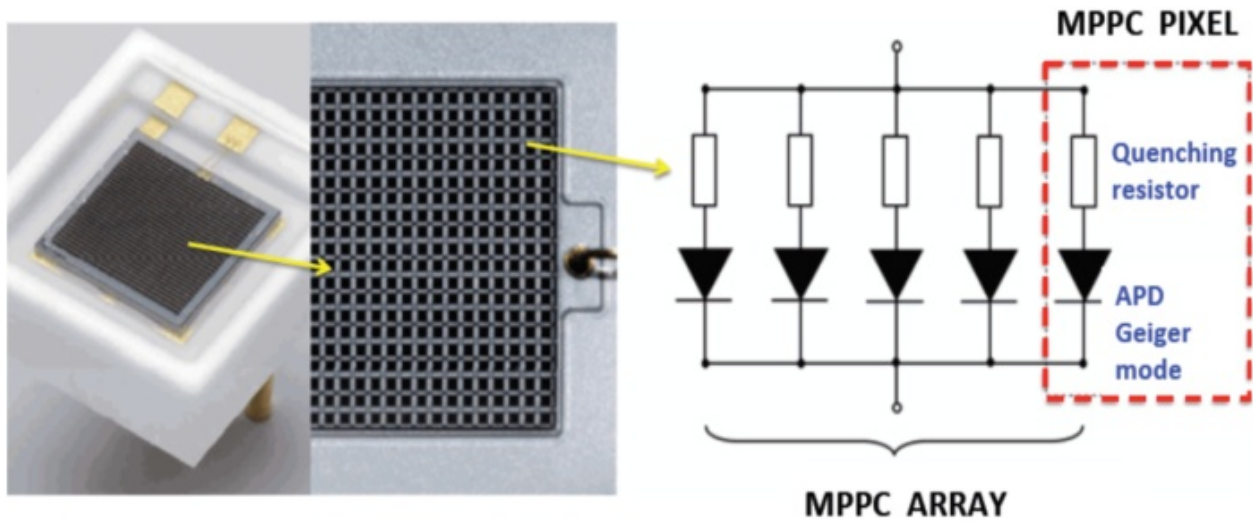


FIGURE 1. (Left) Photograph of a SiPM or Multi-Pixel Photon Counter (MPPC) of $1 \times 1 \text{ mm}^2$ sensitive area divided into hundreds or thousands of APD pixels, (Right) electronic scheme of the array of APDs or individual pixels of the SiPM

SiPMs as other silicon-based detectors have a temperature dependent response to incident light, which is stronger than for conventional PMTs. This temperature dependence of SiPMs can induce considerable uncertainties in the photon measurements and therefore in the dose measurement in scintillation dosimetry. One possible solution to this temperature dependent response is to keep the gain constant, at its nominal value during the measurements, by controlling and maintaining constant the working temperature. Another possibility is dynamically controlling the bias voltage of the SiPM to compensate for temperature variations during the photodetector operation. In this case, a precise characterization of the SiPM gain as a function of temperature and over-voltage is necessary. We have implemented the latter solution at Instituto de Física Corpuscular (IFIC) laboratory, using a thermal humidity test chamber described in Fig.2, in which were set up the following elements:

- A SiPM connected to a printed circuit card (PCB), containing the bias circuit of the photosensor and an operational amplifier, which amplifies and converts the current output of the SiPM into a voltage pulse, suitable for its acquisition and analysis in an oscilloscope. The SiPM used is from Hamamatsu Photonics [8] model S13360-1375CS, with a ceramic package, a typical gain of $G = 4.10^6$ at 25°C , an effective photosensitive area of $1.3 \times 1.3 \text{ mm}^2$ divided into 285 pixels with 82% fill factor.

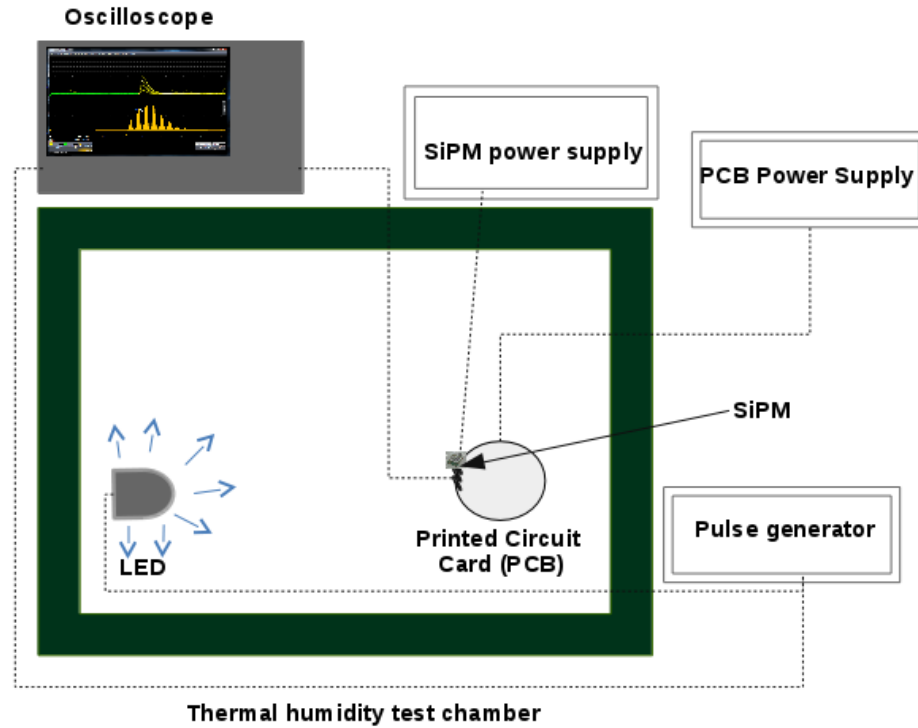
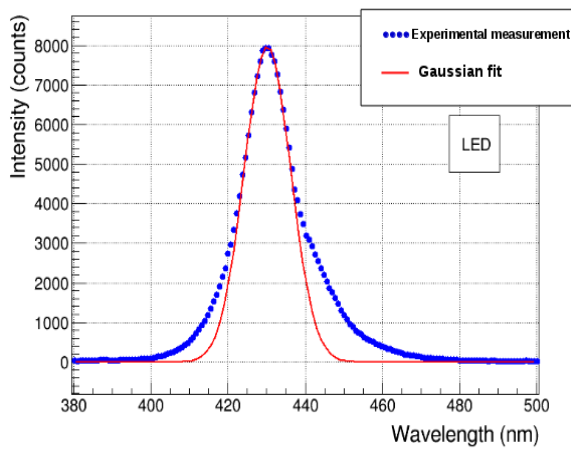
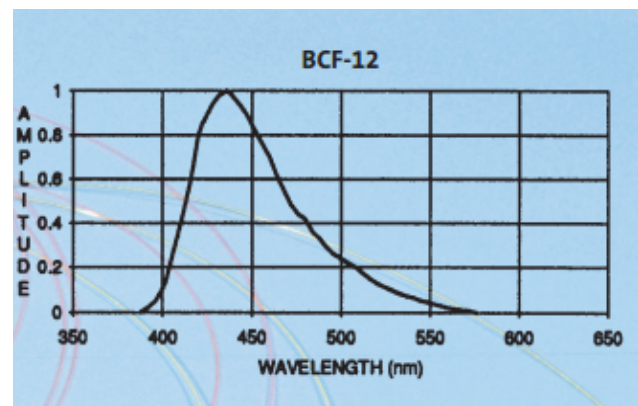


FIGURE 2. Scheme of the experimental setup used for the SiPM gain study

- A Light emitting diode (LED) source (from Roithner Laser Technik GmbH), emitting photons at a wavelength of 430 nm, which corresponds to the peak in the photon emission spectrum of the scintillating fiber BCF12 [9] used in this work. We have indeed measured the light spectrum of the LED as shown in Fig. 3 (a) using a spectrometer, and found it comparable to that emitted by the BCF12 scintillating fibers shown in Fig. 3 (b). The light intensity from the LED is proportional to its polarization current.



(a)



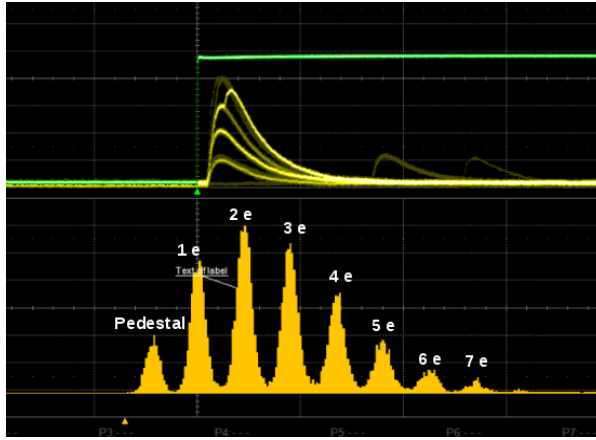
(b)

FIGURE 3. (a) Emission spectrum of the LED we measured using a spectrometer at Instituto de Ciencia Molecular (ICMOL, University of Valencia), (b) Emission spectrum of a scintillating fiber BCF-12 manufactured by Saint Gobain [9]

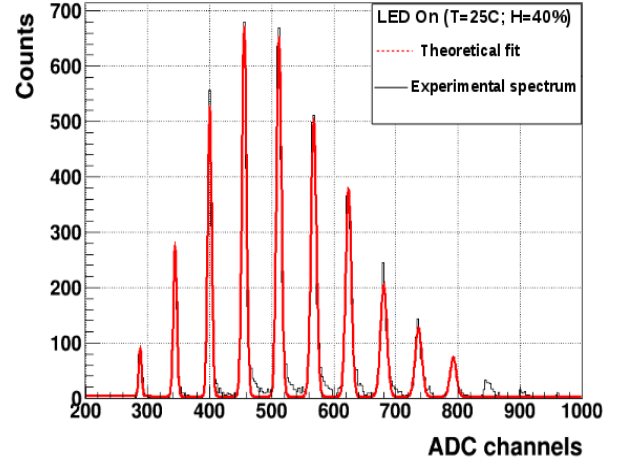
The range of temperatures and voltages used in this study are:

- Temperature range in the test chamber [15°C-41°C], with 15°C being the minimum temperature allowed by the control system of the chamber. This temperature range is that expected in real working conditions of the dosimeter.
- Operating voltage range [51.57V - 55.97V]. Within this range, the operating voltage $V_{OP} = 53.97V$ recommended by Hamamatsu for our SiPM, which ensures a gain of $4 \cdot 10^6$ at 25°C. This bias voltage corresponds to an overvoltage $V_{OV} = 3V$ above the breakdown voltage $V_{BD} = 50.97V$ of the SiPM, provided by the Company (i.e. $V_{OP} = V_{BD} + V_{OV}$).

The LED is used in pulse mode and is set up in front of the SiPM which current signal output is amplified with a gain of $G_{PCB} = 170$, and converted into a voltage pulse. At a given temperature and operating voltage, the oscilloscope records the response of the SiPM, in coincidence with the synchronization signal from the Pulse Generator that feeds the LED. The integration of the pulse voltages in a time window of 500 ns provides the charge spectrum of the SiPM as shown in Fig.4(a). In this figure, peaks of the charge spectrum represent the charge of the SiPM signal for different number of pixels fired at the same time. The first one corresponds to zero charge and it is the ADC pedestal, the other peaks correspond to 1, 2 ...n pixels fired. Using ROOT Data Analysis Framework [10], peaks are fitted to Gaussians, obtaining the mean values of each one and the distances between peaks as shown in Fig. 4 (b).



(a)



(b)

FIGURE 4. (a) Capture from the oscilloscope of the SiPM voltage pulses recorded, and the corresponding charge spectrum obtained by integration of the pulses in a time window of 500 ns. (b) Typical charge spectrum of the SiPM obtained with a LED light source, recorded with the oscilloscope, and fitted using ROOT analysis framework.

The gain can be obtained applying the following expression:

$$G = \frac{\Delta_{\text{peak}}}{R \cdot e} \left[\frac{V}{\text{Ohm.C}} \right] \quad (1)$$

Where R represents the input impedance (50Ω) of the oscilloscope, e is the elementary charge and Δ_{peak} is the mean distance between two successive charge peaks. The gain G in our case is that of the SiPM and the operational amplifier. The SiPM gain is:

$$G_{\text{SiPM}} = \frac{G}{G_{\text{PCB}}} \quad (2)$$

The most correct way to measure the gain is determining the slope of the linear fit to the mean charge as a function of the number of pixels N_p fired in the SiPM, as shown in Fig. 5 and indicated by Eq. (3). The gain uncertainty is determined from the slope uncertainty. The mean charge is provided in Volt ns as a result of integration of the pulse signals in the oscilloscope

$$\text{Mean charge (V ns)} = GN_p + Q_0 \quad (3)$$

Where G is the total gain ($G = G_{\text{SiPM}} \cdot G_{\text{PCB}}$) and Q_0 the charge corresponding to the pedestal.

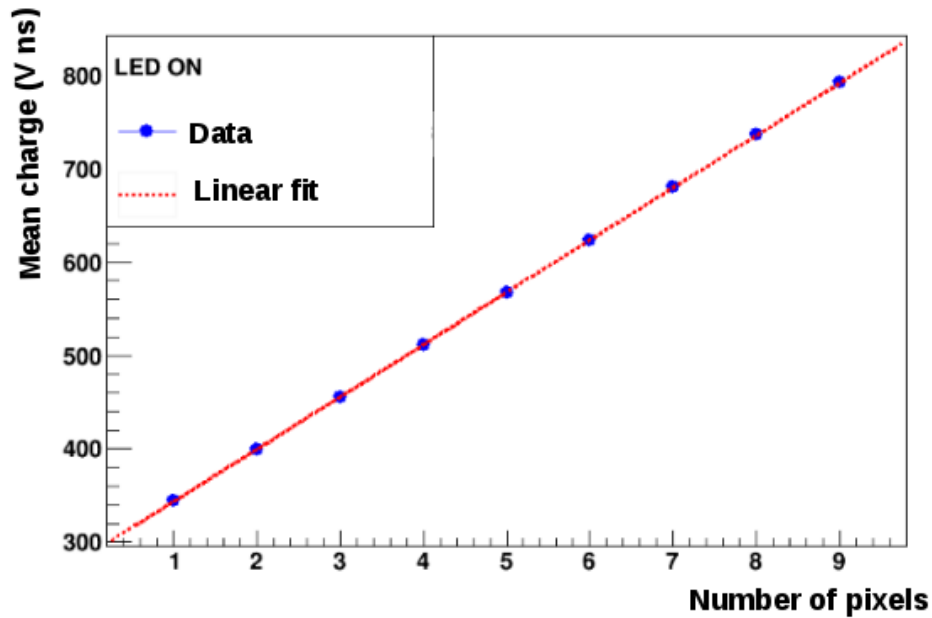


FIGURE 5. SiPM charge as function of the number of pixels fired

Scintillating Fibers: Light Collection Study

Scintillating fibers (SF) are composed of a polystyrene-based core doped with fluorescent molecules, where the scintillation light is produced after a particle energy deposition, and a PMMA cladding. The cladding has lower refractive index than the core to allow total internal reflection and transmission of the scintillation light [9]. Multi-clad fibers have a second cladding layer with even lower refractive index and, thus, allows a total internal reflection at a second boundary. The cladding ensures also the protection of the core from external agents, but may absorb part or the total energy of very low energy radiation. Therefore, the selection of the appropriate scintillation fibers for the design of a detector will depend on the specific application. In this work, we characterized different types of scintillating fibers of 1 mm diameter, model BCF12 from Saint-Gobain [9]: SF without cladding or no-clad fibers (NCF), single-clad fibers (SCF), and multi-clad fibers (MCF). The aim of the present study is the comparison of the light transmission of these different types of SF for their use as a detection medium in a dosimeter for brachytherapy, and the evaluation of the dispersion in light transmission in samples of the same type.

As optical fibers, scintillating fibers transmit light signals from a light source to a light measurement device. We measured the light transmission of the fibers of type NCF, SCF and MCF using the experimental setup shown in Fig. 6. We used as a light source the blue LED used in the experimental setup for the SiPM characterization shown in Fig. 2. The SF is coupled to the LED from one end and to a PMT from the other end, through a fiber connector and a collimator. Optical grease is used between the fiber end and the light or photosensor device. The light spectrum of the LED is similar to that emitted by the SF as shown in Fig. 3. Its intensity, which is proportional to its polarization current, is thoroughly controlled with the source-meter used for its polarization in current mode. The PMT (model R8520 from Hamamatsu Photonics) is calibrated by the manufacturer for quantum efficiency (Q_{eff}) as a function of wavelength. The PMT was biased at its first dynode only with the other dynodes short-circuited. The PMT was thus operated without gain in order to directly measure the photocurrent from incident light on the PMT window, and thus the number of incident photons from the SF. The photocurrent, in the nA range, was measured using an electrometer. The dark photocurrent I_{dark} (in absence of light) of the PMT was measured prior to the light measurement and was subtracted to the total photocurrent I .

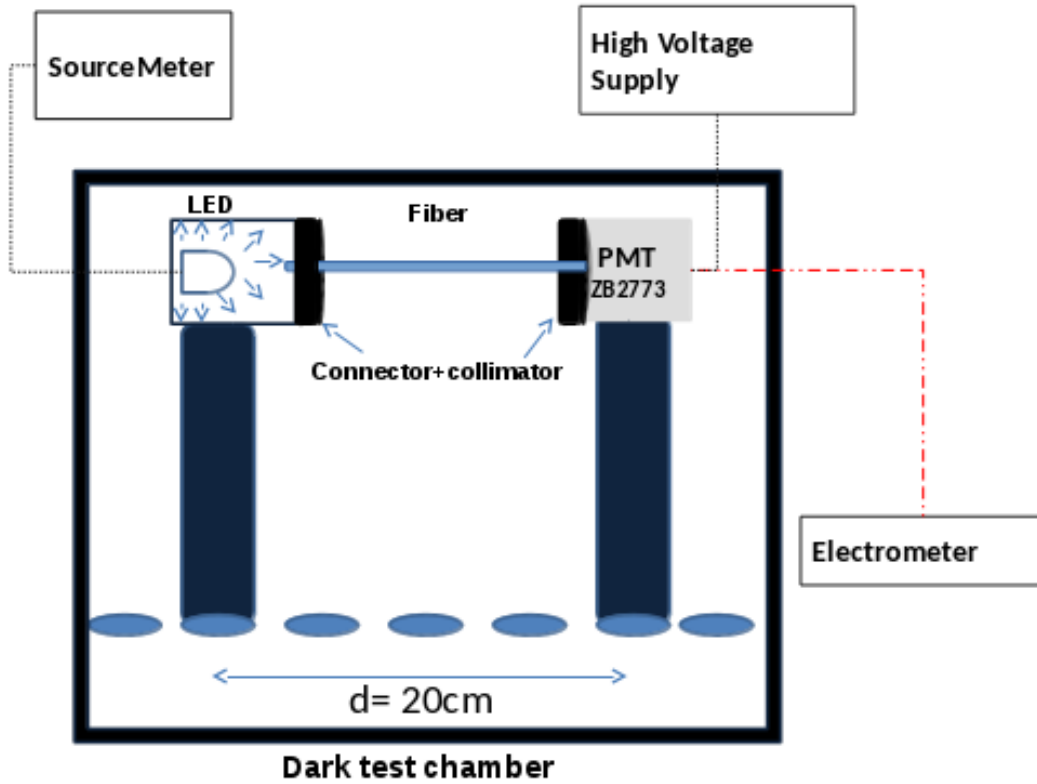


FIGURE 6. Scheme of the experimental setup used for light transmission characterization of scintillating fibers

Prior to the measurements, both ends of the SF were cut with a special guillotine cutting-device for SF manufactured in the laboratory and were polished with various types of polishing films. For each type of BCF12 fibers, ten samples of length 20 cm were prepared for a statistical study of the light transmission in the SF. We used these statistics to draw the relative dispersion of the light transmission in different fibers. The number of photons per nanosecond transmitted by the fiber is calculated using the following expression:

$$N_{photons} = \frac{I - I_{dark}}{Q_{eff}} \quad (4)$$

Where I is the PMT current, with the LED switched on, measured with the electrometer I_{dark} is the PMT current measured in the dark (dark current) and $Q_{eff}= 28.66\%$ is the quantum efficiency of the PMT at the LED peak emission wavelength.

RESULTS AND DISCUSSION

From the measurement procedure described in the experimental setup for the SiPM gain characterization, we plot the gain values as a function of temperature and as a function of operating voltage as shown in Fig. 7 (a) and (b). As seen in Fig. 7(a), the SiPM gain increases linearly with the operating voltage. We can write the gain as:

$$G(V) = a V + b \quad (5)$$

$$\text{Where } a = (1.377 \pm 0.015)10^6 V^{-1} \text{ and } b = -(7.022 \pm 0.081)10^7.$$

On the other hand, the gain decreases linearly with the temperature, so we can write:

$$G(T) = c T + d \quad (6)$$

$$\text{Where } c = -(8.253 \pm 0.159)10^4 C^{-1} \text{ and } d = (6.177 \pm 0.045)10^6.$$

Observing Fig. 7, we notice that the gain variations due to temperature changes can be compensated with an appropriate variation of the bias voltage i.e. when we increase the temperature in the chamber we can also increase the operating voltage to keep the gain constant, and vice versa.

At $25^\circ C$ we found the SiPM gain $G = (4,21 \pm 0,04)10^6$ while the value provided by Hamamatsu is 4.10^6 . From extrapolation at $G(V_{BD})=0$ we obtain the break-down voltage of the SiPM $(V_{BD})_{exp} = 50.99$ V. The value given by Hamamatsu is $V_{BD}=50.97V$, which shows a very good agreement with our measurements within 0,04 %.

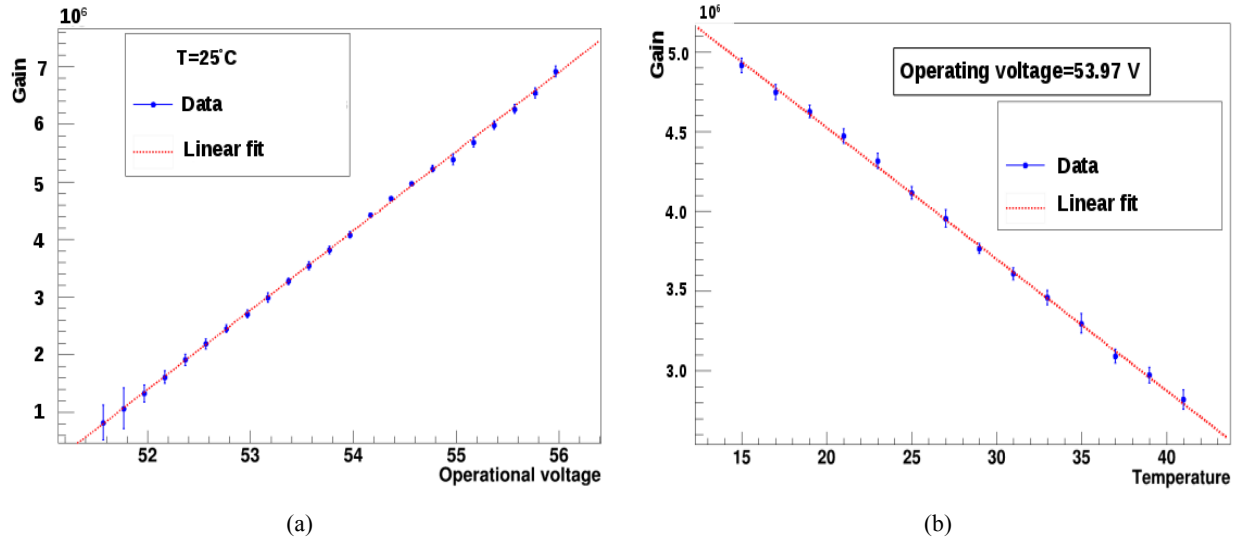


FIGURE 7. SiPM Gain as a function of operating voltage (a) and temperature within the range of interest in clinical use of the photosensor (b)

From equations (5) and (6) we draw the bias voltage correction per unit of temperature on the SiPM bias voltage necessary to stabilize its gain during operation at room temperature:

$$\Delta V = \alpha \Delta T \quad (7)$$

$$\alpha = -\frac{c}{a} = (0.0599 \pm 0.0013) \frac{V}{^{\circ}C} \quad (8)$$

Taking as a reference bias voltage, the nominal voltage provided by Hamamatsu for the operation of the SiPM at $T_{ref}=25^{\circ}C$: $V_{ref} = V_{BD} + 3V = 53.97V$, for which the SiPM gain measured is $G = 4.20 \cdot 10^6$, the voltage bias as a function of temperature that has to be applied for stabilizing the SiPM gain is:

$$V = \alpha T + \beta, \text{ where } \alpha = (59.9 \pm 1.3) mV \text{ and } \beta = (52.47 \pm 0.03)V \quad (9)$$

This procedure of temperature dependent voltage bias of the SiPM may be implemented in a feedback voltage supply circuit using a digital temperature sensor for temperature measurement at the photosensor location.

In order to evaluate the stability of the gain using this voltage compensation procedure, we measured the SiPM gain for a range of temperatures between $21^{\circ}C$ and $29^{\circ}C$ with a step of $2^{\circ}C$, while correcting the bias voltage of the SiPM by $\sim 60 mV/^{\circ}C$ to maintain its gain at the nominal value of $(4.21 \pm 0.06)10^6$ at $25^{\circ}C$. Fig. 8 represents the SiPM gain after implementation of the voltage correction as a function of temperature. The red line corresponds to the fit of the data with a straight line ($G(T) = G_0 + G_1 T$, where $G_1 = 7.826 \cdot 10^3 ^{\circ}C^{-1}$ and $G_0 = 3.999 \cdot 10^6$). The maximum relative variation of the gain obtained in the large range of temperatures considered ($21-29^{\circ}C$) is 0.9 %, which indicates that the gain is precisely stabilized at its nominal value at $25^{\circ}C$.

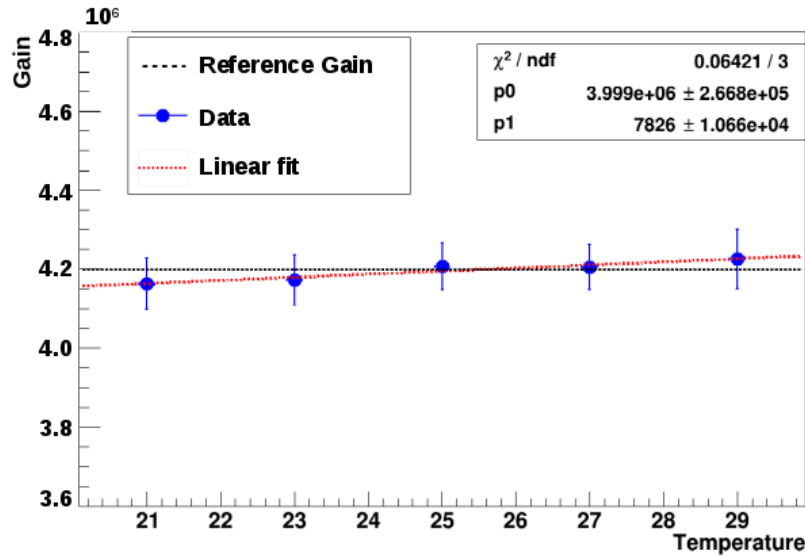


FIGURE 8. Gain curve as a function of temperature after implementation of the voltage compensation ($\sim 60 mV/^{\circ}C$) for the gain drift correction in the SiPM

From the measurement procedure described for the scintillating fibers study, we observe that the number of photons transmitted by the SF per unit of time, measured by the PMT, increases linearly with the light intensity from the LED (which is proportional to its polarization current I_{LED}) as shown in Fig. 9. In Fig. 9 (a) where this plot is shown for a sample of ten SF of the same type (BCF12 single-clad), the relative dispersion is of 7% around the mean, due to the uncertainties in the manufacturing process and in the measurements procedure on the laboratory. The same measurements of samples of ten SF of other types (multi-clad and no-clad) have been performed and are plotted in Fig. 9(b). This figure shows that at the same light intensity, single-clad fibers have higher light transmission compared to multi-clad and no-clad fibers of the same diameter (1 mm). These preliminary measurements indicate that, with the same external diameter of the SF (1 mm), the second cladding does not improve the light collection because of a smaller core for the same input light intensity. Thus, the increase of light collection

announced by the manufacturer (Saint-Gobain) for multi-clad SF of up to 60% [9] has to be interpreted with care. However, during the preparation and work with these SF (cutting, polishing, manipulating), we noticed that the second cladding adds substantial mechanical strength to the fibers. This feature may be essential for small scintillation dosimeter (few mm length), at the expense of lower light collection, if the scintillation yield and the SiPM gain and photodetection efficiency are high enough.

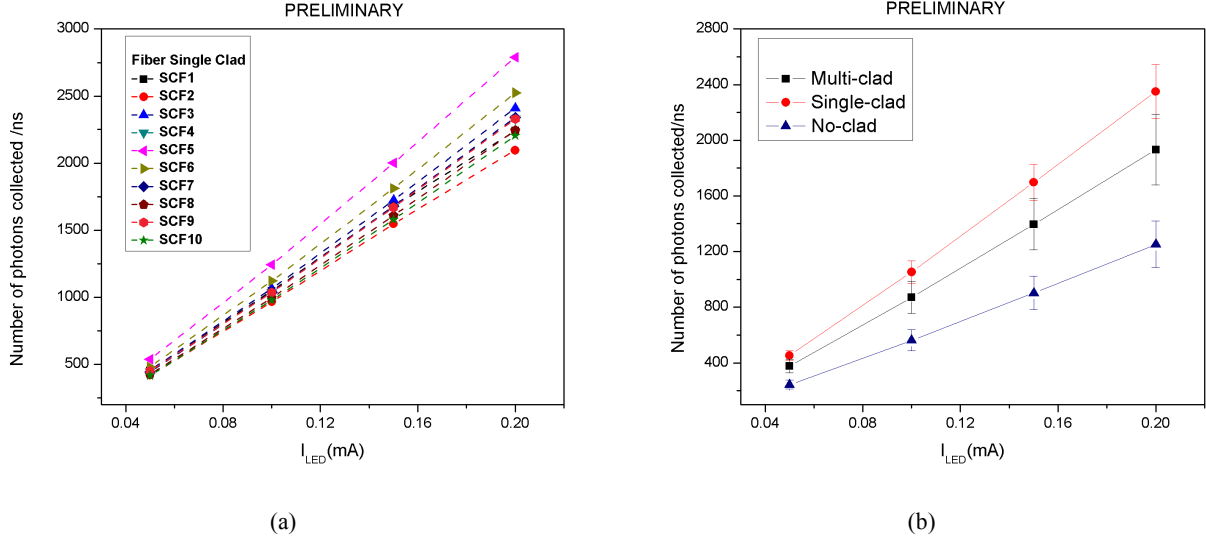


FIGURE 9. (a) Number of photons transmitted per nanosecond as a function of the LED polarization current in ten samples of a SF of the same type BCF12 single-clad, (b) Mean number of photons transmitted by ten scintillating fibers BCF12 of three types as a function of the LED polarization current.

CONCLUSION

The design and construction of a scintillation dosimeter for brachytherapy, requires the precise characterization of all its components. The dosimeter prototype which we are characterizing is composed of a scintillation fiber, an optical light guide, a SiPM and its readout electronics. In this workpaper, we have presented the experimental studies performed on the gain stabilization of the SiPM and the preliminary measurements of the light transmission in different types of fibers.

We have shown that it is possible to stabilize the SiPM gain at its nominal value (at 25°C), against variations of the temperature, with a precision of 0.9% over a large range of temperatures (21-29°C). This stabilization of the gain, which will be implemented electronically and automatically in the polarization circuit of the SiPM, is a major issue for a stable and precise in-vivo measurement of the radiation dose in brachytherapy.

When a charged particle deposits its energy in the scintillator, optical photons are emitted isotropically. An important property of the scintillator emission is the scintillation yield given by the manufactory, it represents the number of photons emitted per MeV (8000 photons/MeV for BCF-12[9]). In our project, we will use Cobalt-60 (1.173MeV and 1332MeV) source to generate optical photons in the fiber where the energy deposition is mainly done by Compton effect, the number of photons is < 8000. The transmission of these photons by scintillation fibers is shown to increase linearly.

Single-clad fibers are shown to have higher light transmission than no-clad and multi-clad fibers of the same external diameter, which could make them the best choice for an in-vivo dosimeter. However, multi-clad fibers have stronger mechanical strength and could be the best compromise between high light transmission and best mechanical properties for a point-like scintillation dosimeter. The statistical study on a sample of 10 fibers indicates a dispersion

of 7% due to the uncertainties in the manufacturing process and in the measurements procedure. These preliminary results should be confirmed by further measurements.

ACKNOWLEDGMENTS

This work is part of a doctoral project, proposed within the collaboration between IFIC and Valencia University and University USTHB of Algiers (Algeria). We acknowledge all members of SNIRM laboratory (USTHB), IFIC (CSIC-University of Valencia), the Laboratorio de Radiactividad Ambiental of University of Valencia and the IFIMED, the funding from Catedra UNESCO of the General Foundation of the University of Valencia and also the funding from IFIC through the Severo Ochoa grant. N.H. Boughaba acknowledges the Algerian MERS for her doctoral fellowship.

REFERENCES

1. M. J. Rivard, J. P. Calatayud, F. Ballester, R. K. Das, Z. Ouhib. "Dose calculation for photon-emitting brachytherapy sources with average energy higher than 50 keV: Report of the AAPM and ESTRO", update Medical Physics, Vol. 39, No. 5, May 2014
2. G. Kertzscher, A. Rosenfeld, S. Beddar, K. Tanderup, J.E. Cygler. "In vivo dosimetry: trends and prospects for brachytherapy". Vol. 87. May 2014
3. S. Beddar and L. Beaulieu. "Basic principles and theory" in Scintillation Dosimetry (Taylor & Francis Group 2016), pp. 53-71
4. S. Beddar. "Radiation Response of Optical Fibers to Clinical Radiotherapy Photon and Electron Beams" in Paris OPTO 1988: ESI Publications) pp. 146-9
5. S. Beddar, T. Mackie, F. H. Attix. "Water-Equivalent Plastic Scintillation Detectors for High-Energy Beam Dosimetry: I. Physical Characteristics and Theoretical Consideration". Physics in Medicine and Biology 37, N°10 (October 1992), pp. 1883-1900
6. S. Beddar. "A new scintillator detector system for the quality assurance of Co-60 and high-energy therapy machines", Physics medical and biology. Vol. 39, 1994, pp. 253-63
7. S. Beddar. "Water equivalent plastic scintillation detectors in radiation therapy" in Radiation Protection Dosimetry (2006), Vol. 120, No. 1-4, pp. 1-6
8. Hamamatsu, MPPC (Multi Pixel Photon Counter), <https://www.hamamatsu.com>
9. Saint-Gobain Crystals, <https://www.crystals.saint-gobain.com>
10. ROOT Data Analysis Framework, <https://root.cern.ch>